

AN INTELLIGENT CONTROL POLICY FOR FUEL INJECTION CONTROL OF CNG ENGINES*

F. BARGHI AND A. A. SAFAVI**

School of Electrical and Computer Eng., Shiraz University, Namazi Sq., Shiraz, 71348-51154, I. R. Iran
Email: safavi@shirazu.ac.ir

Abstract– This paper proposes an intelligent control technique for fuel injection control of Compressed Natural Gas (CNG) engines. Recurrent Neuro-Fuzzy Networks are used to estimate and control air to fuel ratio (AFR) of CNG engines. To reasonably handle such a complicated control problem, a precise experimental test has been done on a real CNG fuelled vehicle and the process input output data have been collected by running the vehicle in transient conditions. To determine the proper amount of gas to be injected, a controller has been designed based on nonlinear inverse dynamics of AFR. The results show that the predicted results are in line with the measured fuel injection commands produced by the real electronic control unit (ECU). This evaluated and validated the efficiency of the controller. The control strategy has the advantage that control actions can be calculated analytically, avoiding the costly and time-consuming calibration efforts required in conventional fuel injection control strategies.

Keywords– Fuel injection control, CNG engine, recurrent Neuro-Fuzzy networks

1. INTRODUCTION

In recent years, there has been a continuing effort to reduce fuel consumption and emissions of car engines due to the serious environmental effects and the lack of common fossil fuels [1, 2]. A key solution to face these problems is to control the fuel to be injected to the engine. Indeed, an accurate amount of fuel to be injected in the appropriate air/fuel mixture strictly depends on the fuel properties and the applied control strategy. The conventional car fuel injection controllers are based on static 3D maps and are designed in part with classical P and PI controllers to control the air to fuel ratio [3, 4]. Since this strategy needs high calibration efforts with quite costly and time-consuming experiments, spaces are opened for new contributions to improve the control performance with less calibration effort [5, 6]. For this purpose, particular interests have been dedicated to engine modeling and control [7-10]. Identification techniques [11] and adaptive control methodologies have been proposed in order to identify and estimate the states and tune the parameters with the aid of real-time measurements (e.g. Observers, Kalman filters) [12-15]. Robust control (especially H_∞ control) [16-18] and Sliding mode control [19] methodologies have also attracted attention for this problem. Another promising solution for approaching this problem is given by intelligent techniques such as Neural Networks and Fuzzy Logic Systems [20]. In [21-23], authors have investigated the Recurrent Neural Network models for AFR estimation and control in SI engines. They have reproduced the target patterns with satisfactory accuracy. But the major problem of this procedure is the trial and error practice to find the appropriate number of hidden layers and the proper number of nodes in each layer. A radial basis function (RBF) neural network based approach for the fuel injection control problem and a linear model predictive control (MPC) scheme for maintaining the AFR near the

*Received by the editors September 29, 2010; Accepted June 5, 2012.

**Corresponding author

stoichiometric value are found in [24, 25]. Nevertheless, an engine works in a wide operating region and a linear model is only valid for a small region around a specific operating point. Fuzzy Logic Systems are also used in [26-29] to achieve the regulation of the fuel injection system of SI engines. Although the results show considerable improvements in fuel injection regulation, the parameters of the fuzzy control paradigm are a collection of rules and fuzzy-set membership functions that are intuitively comprehensible by the operator. This approach is much harder when the number of inputs, membership functions and rules increase.

The fuel properties also have a major effect on combustion and emissions [30-33]. From the environmental viewpoint, CNG engines guarantee cleaner combustion than conventional gasoline and diesel engines due to the much smaller amount of nitrogen oxides (NO_x) and carbon dioxide (CO₂) emissions. In [34], authors have investigated the various aspects of CNG engines in more detail. In this study, to face the issues associated with the fuel injection control of CNG engines, an intelligent modeling of AFR is proposed and based on this model a fuel injection controller is designed. The results show that the response of controller is quite similar to the measured fuel injection commands produced by the real ECU, but with less calibration effort. This indicates the efficiency of the controller.

This paper is structured as follows. Section 2 describes potentials of the intelligent technique for AFR estimation and control. Section 3 and 4 explain the RNFN design method for AFR estimation and control. In Section 5, the details of the experimental test are given. The modeling and control results are shown in Section 6. Finally, Section 7 concludes this paper.

2. POTENTIALS OF RECURRENT NEURO-FUZZY NETWORKS FOR AFR ESTIMATION AND CONTROL

Fuzzy Logic Systems have many good features such as high mapping capability, handling nonlinear dynamics, flexibility and reliability. Nevertheless, they also have many design parameters that may take a very long time to design, tune and debug. Besides, the number of fuzzy if-then rules is proportional to both the number of membership functions in the fuzzy sets and the number of input variables; it may also be difficult to determine the rules when the resulting number of rules is extremely high. The learning capability of Neural Networks, especially the multi-layer perceptrons (MLPs) [35] has also attracted attention for developing various prediction models, due to its flexibility and universal approximating capability [36-37]. Recently, interest in using Recurrent Neural Networks (RNNs) has become a popular approach for the identification and control of temporal problems. The RNNs are MLP Networks with feedback connections among the neurons to introduce a dynamic effect in their computational system [38]. Even though MLP and RNN networks with back propagation learning seem to be very convenient to design, networks such as black-box models may not be easy to debug [39]. To provide better results in identifying and controlling non-linear dynamical systems and to inherit most common characteristics of both FLSs and RNNs, the Recurrent Neuro-Fuzzy Networks (RNFN) are preferred [40-42]. The RNFN is a Neuro-Fuzzy Network [43-45] with feedback connection between the neurons located in the output and input layers of the Network. It has the following special features. RNFN is comprised of If-Then statements that are easier to understand while its structure is not of the black-box nature of neural networks, thus it can be more easily debugged [39]. It is fundamentally based on Neuro-Fuzzy Networks that have been mathematically introduced in the literature and have unlimited approximation power for matching any nonlinear function arbitrarily well [46]. It also learns the rules from real collected samples which ease the design process. RNFN has fewer parameters to be determined than NN. Therefore, it can provide faster training without loss of generalization power [45, 46].

This research is distinctive in terms of using a RNFN structure as an intelligent approach for both modeling and control of AFR in CNG engines in order to limit the AFR excursions from stoichiometry at different operational regions. Besides, the design is based on real data collected from a real car and the results are compared with the real outputs of the ECU.

3. RNFN FOR AFR ESTIMATION

To build a model for nonlinear dynamics of AFR, consider the following NARX model:

$$y(t) = \mathbf{F} [y(t-1), y(t-2), \dots, y(t-n), u(t), u(t-1), \dots, u(t-m), s(t), s(t-1), \dots, s(t-m)] \quad (1)$$

where y , u and s are output, input command and input variables, respectively. Indices n and m are the lag spaces. Generally, the determination of mapping function F is not a trivial task. To overcome this problem a RNFN structure as shown in Fig. 1 can be used.

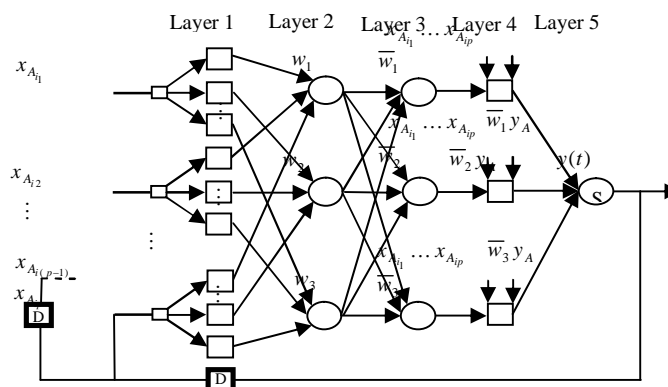


Fig. 1. RNFN Structure (each circles indicate a fixed node, squares are adaptive nodes and “D” block denote a lag space)

In this structure, 's' are the linguistic variables consisting of output, input command and input variables (as are discussed in Section 5); where i is the number of samples and p is the number of linguistic variables. To produce a concise representation of the process behaviour, the measured input-output data which span most of the engine operating regions are clustered into several fuzzy operating regions. Within each region, a local linear model is used to represent the process behaviour and the global model output is obtained through the defuzzification related to K fuzzy clustered regions; each variable has k fuzzy sets $inpmfk$ ($k = 1, 2, \dots, K$). Fuzzy sets are used to define process operating regions such that the fuzzy dynamic model of a nonlinear process can be described in the following way:

Rule k : IF (is in $in1mfk$) and (is in $in2mfk$) and ... and (is in $inpmfk$) THEN

$$y_{A_k} = a_{k1}x_{A_{i1}} + a_{k2}x_{A_{i2}} + \dots + a_{kp}x_{A_{ip}} + b_k$$

where 's' are outputs within the fuzzy clustered regions specified by the fuzzy rules and 's' and 's' are design parameters. To set up the membership functions and to determine the parameters, process input output data are used to train the RNFN network. Through training, membership functions of fuzzy clustered regions are refined and local models are learned.

In Fig. 1, each circle indicates a fixed node, whereas a square indicates an adaptive node and “D” block denotes a lag space. Similar functions are allocated to nodes in the same layer. Output of nodes in layer l is denoted as $y_{A_{lh}}$ where l is the layer number and h is neuron number of the next layer. The function of each layer is described as follows:

Layer 1: The outputs of this layer are the fuzzy membership grade of the inputs. In this application, 14 inputs are chosen to estimate the AFR nonlinear dynamics and 3 membership functions related to 3 fuzzy operating regions are assigned to each input. Hence, 42 outputs are given by:

$$\begin{aligned} O_h^1 &= \mu_{A_h}(x_{A_{11}}), h=1,2,3 \\ O_h^1 &= \mu_{A_{h-3}}(x_{A_{12}}), h=4,5,6 \\ &\vdots \\ O_h^1 &= \mu_{A_{h-39}}(x_{A_{14}}), h=40,41,42 \end{aligned} \quad (2)$$

where $\mu_{A_h}(x_{A_{11}}), \dots, \mu_{A_{h-39}}(x_{A_{14}})$ could adopt any fuzzy membership function. For example, if the bell shaped membership function is employed, it is given by:

$$\mu_{A_h}(x_{A_{11}}) = \frac{1}{1 + \left[\left(\frac{x_{A_{11}} - r_h}{p_h} \right)^2 \right]^{q_h}}, \quad h=1,2,3 \quad (3)$$

where p_h , q_h and r_h are the parameters of the membership function, governing the bell shaped functions accordingly.

Layer 2: Each node computes the firing strengths of the associated rules. The output of nodes in this layer can be presented as:

$$O_h^2 = w_h = \mu_{A_h}(x_{A_{11}}) \mu_{A_{h+3}}(x_{A_{12}}) \dots \mu_{A_{h+39}}(x_{A_{14}}), h=1,2,3 \quad (4)$$

Layer 3: In the third layer, the nodes are also fixed nodes. They play a normalization role to the firing strengths from the previous layer. The outputs of this layer can be represented as:

$$O_h^3 = \bar{w}_h = \frac{w_h}{w_1 + w_2 + w_3} \quad (5)$$

Layer 4: The output of each adaptive node in this layer is simply the product of the normalized firing level and a first order polynomial of a Takagi-Sugeno model. Thus, the outputs of this layer are given by:

$$O_h^4 = \bar{w}_h y_{A_k} = \bar{w}_h (a_{k1} x_{A_{11}} + a_{k2} x_{A_{12}} + \dots + a_{k14} x_{A_{14}} + b_k), h=k=1,2,3 \quad (6)$$

Layer 5: Finally, in layer 5, the circle node S sums all incoming signals. Hence, the overall output of the model is given by:

$$O_h^5 = \sum_{h=1}^3 \bar{w}_h y_{A_k} = \frac{\sum_{h=1}^3 w_h y_{A_k}}{w_1 + w_2 + w_3}, h=k=1,2,3 \quad (7)$$

The RNFN has two adaptive layers, the first layer with modifiable parameters p_h , q_h and r_h and the fourth layer with modifiable parameters a_{k1}, \dots, a_{k14} and b_k . The task of the learning algorithm is to tune all these modifiable parameters to make the network output match the training data. Substituting the fuzzy if-then rules into (7), it becomes:

$$\begin{aligned} y &= \bar{w}_1 (a_{11} x_{A_{11}} + a_{12} x_{A_{12}} + \dots + a_{114} x_{A_{14}} + b_1) + \bar{w}_2 (a_{21} x_{A_{11}} + a_{22} x_{A_{12}} + \dots + a_{214} x_{A_{14}} + b_2) + \\ &\bar{w}_3 (a_{31} x_{A_{11}} + a_{32} x_{A_{12}} + \dots + a_{314} x_{A_{14}} + b_3) \end{aligned} \quad (8)$$

After rearrangement, the output can be expressed as:

$$y = (\bar{w}_1 a_{11})x_{A_{i1}} + (\bar{w}_1 a_{12})x_{A_{i2}} + \dots + (\bar{w}_1 a_{114})x_{A_{i14}} + (\bar{w}_1)b_1 + (\bar{w}_2 a_{21})x_{A_{i1}} + (\bar{w}_2 a_{22})x_{A_{i2}} + \dots + (\bar{w}_2 a_{214})x_{A_{i14}} + (\bar{w}_2)b_2 + (\bar{w}_3 a_{31})x_{A_{i1}} + (\bar{w}_3 a_{32})x_{A_{i2}} + \dots + (\bar{w}_3 a_{314})x_{A_{i14}} + (\bar{w}_3)b_3 \quad (9)$$

which is linear in the parameters a_{k1}, \dots, a_{k14} and b_k . The parameters associated with the membership functions change through the learning process. The computation and adjustment of these parameters are facilitated by a gradient vector. This gradient vector provides a measure of how well the fuzzy inference system models the input output data for a given set of parameters. When the gradient vector is obtained, any of the several optimization routines can be applied in order to adjust the parameters to reduce some error measure. This error measure is usually defined by the sum of the squared difference between actual and desired outputs. Here, the premises parameters p_h , q_h and r_h are updated by gradient descent in the backward pass while the consequent parameters a_{k1}, \dots, a_{k14} and b_k are identified by the least-squares method to set up the following fuzzy if-then rules:

- 1) If ($x_{A_{i1}}$ is in_1mf_1) and ($x_{A_{i2}}$ is in_2mf_1) and ($x_{A_{i3}}$ is in_3mf_1) and ($x_{A_{i4}}$ is in_4mf_1) and ($x_{A_{i5}}$ is in_5mf_1) and ($x_{A_{i6}}$ is in_6mf_1) and ($x_{A_{i7}}$ is in_7mf_1) and ($x_{A_{i8}}$ is in_8mf_1) and ($x_{A_{i9}}$ is in_9mf_1) and ($x_{A_{i10}}$ is $in_{10}mf_1$) and ($x_{A_{i11}}$ is $in_{11}mf_1$) and ($x_{A_{i12}}$ is $in_{12}mf_1$) and ($x_{A_{i13}}$ is $in_{13}mf_1$) and ($x_{A_{i14}}$ is $in_{14}mf_1$) then $y_{A_1} = a_{11}x_{A_{i1}} + a_{12}x_{A_{i2}} + \dots + a_{114}x_{A_{i14}} + b_1$
- 2) If ($x_{A_{i1}}$ is in_1mf_2) and ($x_{A_{i2}}$ is in_2mf_2) and ($x_{A_{i3}}$ is in_3mf_2) and ($x_{A_{i4}}$ is in_4mf_2) and ($x_{A_{i5}}$ is in_5mf_2) and ($x_{A_{i6}}$ is in_6mf_2) and ($x_{A_{i7}}$ is in_7mf_2) and ($x_{A_{i8}}$ is in_8mf_2) and ($x_{A_{i9}}$ is in_9mf_2) and ($x_{A_{i10}}$ is $in_{10}mf_2$) and ($x_{A_{i11}}$ is $in_{11}mf_2$) and ($x_{A_{i12}}$ is $in_{12}mf_2$) and ($x_{A_{i13}}$ is $in_{13}mf_2$) and ($x_{A_{i14}}$ is $in_{14}mf_2$) then $y_{A_2} = a_{21}x_{A_{i1}} + a_{22}x_{A_{i2}} + \dots + a_{214}x_{A_{i14}} + b_2$
- 3) If ($x_{A_{i1}}$ is in_1mf_3) and ($x_{A_{i2}}$ is in_2mf_3) and ($x_{A_{i3}}$ is in_3mf_3) and ($x_{A_{i4}}$ is in_4mf_3) and ($x_{A_{i5}}$ is in_5mf_3) and ($x_{A_{i6}}$ is in_6mf_3) and ($x_{A_{i7}}$ is in_7mf_3) and ($x_{A_{i8}}$ is in_8mf_3) and ($x_{A_{i9}}$ is in_9mf_3) and ($x_{A_{i10}}$ is $in_{10}mf_3$) and ($x_{A_{i11}}$ is $in_{11}mf_3$) and ($x_{A_{i12}}$ is $in_{12}mf_3$) and ($x_{A_{i13}}$ is $in_{13}mf_3$) and ($x_{A_{i14}}$ is $in_{14}mf_3$) then $y_{A_3} = a_{31}x_{A_{i1}} + a_{32}x_{A_{i2}} + \dots + a_{314}x_{A_{i14}} + b_3$

4. RNFN FOR AFR CONTROL

Based on the latter RNFN estimator, an inversed model-based predictive controller can be developed. Assume that the NARX model of the AFR estimator is a one step ahead predictor given by (10):

$$y(t+1) = \mathbf{G} [y(t), y(t-1), \dots, y(t-n), u(t), u(t-1), \dots, u(t-m), s(t), s(t-1), \dots, s(t-m)] \quad (10)$$

This assumption allows having a predictive controller by inverting the control and output variables, as (11):

$$u(t) = \mathbf{H} [y(t+1), y(t), y(t-1), \dots, y(t-n), u(t-1), \dots, u(t-m), s(t), s(t-1), \dots, s(t-m)] \quad (11)$$

Replacing the $y(t+1)$ value by the desired value $r(t+1)$ results in the following NARX model for the controller:

$$u(t) = \mathbf{H} [r(t+1), y(t), y(t-1), \dots, y(t-n), u(t-1), \dots, u(t-m), s(t), s(t-1), \dots, s(t-m)] \quad (12)$$

Now a RNFN controller structure can be employed to determine the parameters (Fig. 2). The RNFN training task is performed almost in the same way as the latter RNFN, with the only difference being that the control and output variables are replaced. The controller consists of several local linear model-based

controllers. Local controllers are constructed based on the corresponding local linear models and their outputs are combined to form a global control action.

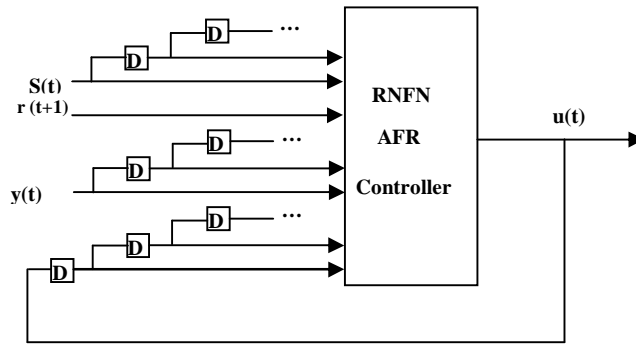


Fig. 2. RNFN-Based AFR Controller schematic representation (“D” block denotes the lag space)

5. EXPERIMENTAL TEST

The experiments have been carried out on a real vehicle (Soren with EF7-TC engine) at the Engine Research Center of Irankhodro Company (IPCO). For measuring the engine variables and simultaneous ECU data acquisition, the high speed data interface ETK and ES590 Interface tools have been used (Fig. 3). The process input output data have been collected by running the vehicle on the test bench in transient conditions. To simulate the real riding situation in the urban areas, the wind force and the road friction are simulated physically at the test bench (Fig. 4).

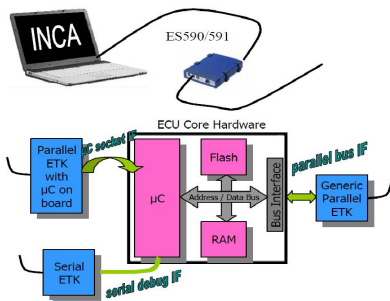


Fig. 3. High speed ECU data acquisition equipment based on ETAS products [47]



Fig. 4. The under study vehicle, embedded equipment, wind force and road friction physical simulator systems

Regardless of cold start conditions, the experimental test is designed based on normal performance of vehicle movement in an urban area. For this test, the engine speed (Fig. 5) is considered between 700 to 3500 RPM. The vehicle speed is a function of several factors such as the engine speed, the loaded tire radius and the transmission gear ratio is between 0 to 70 Km/h (Fig. 6). It can be seen from Fig. 7 that the throttle plate angle varies in the limit range between 0 to approximately 20 degrees. These changes cause the manifold air dynamic excitation and consequently manifold pressure to vary from 200 to 1200 mBar (Fig. 8). The fuel injection duration calculated by ECU for these conditions is shown in Fig. 9. As a result, the air to fuel ratio varies as in Fig. 10. It should be noted that the optimal air to fuel ratio of 14.7/1(stoichiometric value) is often called Lambda=1 or $\lambda=1$ condition. The control strategy must maintain the AFR around $\lambda=1$.

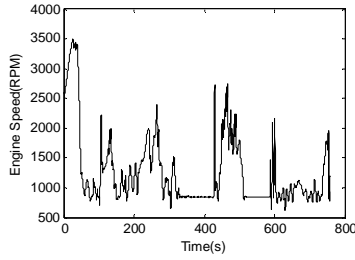


Fig. 5. Engine speed (RPM)

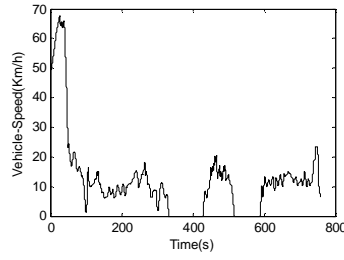


Fig. 6. Vehicle speed (Km/h)

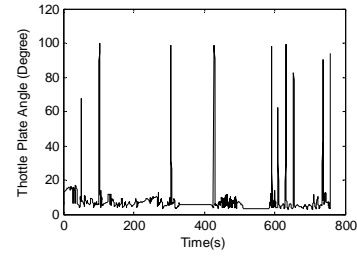


Fig. 7. Throttle plate angle (Degree)

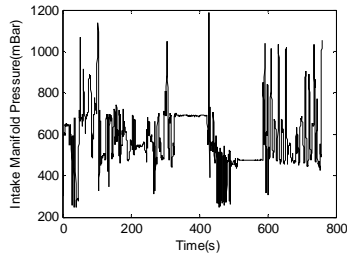


Fig. 8. Intake manifold pressure (mBar)

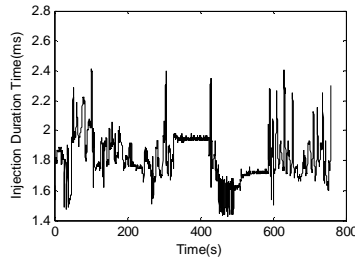


Fig. 9. Injection duration (ms)

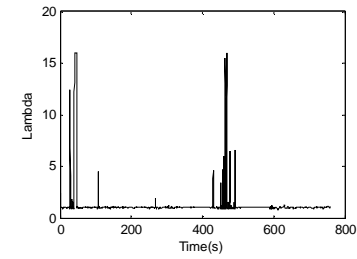


Fig. 10. Air to fuel ratio curve (λ)

6. RESULTS

The goal of employing the RNFN estimator structure in this approach is to model the AFR dynamics for a wide range of engine operating scenarios. Since this work uses the rearranged NARX model for the AFR controller, a RNFN-based controller can be a powerful aid in designing an inverse model based controller. The scope of such control scheme is to keep the AFR constraint conditions by providing the proper fuel injection commands. The RNFN estimation and control strategy utilizes both process knowledge and process input output data. Process knowledge is used to set up the experimental test and to define a NARX model for AFR estimation or control while the process input output data are used to train the network. Depending on this strategy and based on (1), the most effective variables on AFR dynamics are selected to define an appropriate NARX for AFR estimation:

$$AFR(t) = F [AFR(t-1), AFR(t-2), \dots, AFR(t-n), P_{man}(t), P_{man}(t-1), \dots, P_{man}(t-m), rpm(t), rpm(t-1), \dots, rpm(t-m), a_{th}(t), a_{th}(t-1), \dots, a_{th}(t-m), t_{inj}(t), t_{inj}(t-1), \dots, t_{inj}(t-m)] \quad (13)$$

The variables P_{man} , rpm , a_{th} , t_{inj} are manifold pressure, engine speed, throttle plate angle and the fuel injection time duration, respectively. After the correlation tests and selecting $n = 2$ and $m = 2$ for lag spaces, the RNFN estimator structure is defined with 14 inputs and one output.

$$= [AFR(t-1), AFR(t-2), \dots, AFR(t-n), P_{man}(t), P_{man}(t-1), \dots, P_{man}(t-m), rpm(t), rpm(t-1), \dots, rpm(t-m), a_{th}(t), a_{th}(t-1), \dots, a_{th}(t-m), t_{inj}(t), t_{inj}(t-1), \dots, t_{inj}(t-m)] \quad (14)$$

$$y(t) = [AFR(t)]$$

Based upon (12), another NARX model for the AFR controller could be considered as shown below:

$$t_{inj}(t) = H [AFR(t+1), AFR(t), \dots, AFR(t-n), P_{man}(t), P_{man}(t-1), \dots, P_{man}(t-m), rpm(t), rpm(t-1), \dots, rpm(t-m), a_{th}(t), a_{th}(t-1), \dots, a_{th}(t-m), t_{inj}(t-1), \dots, t_{inj}(t-m)] \quad (15)$$

where $AFR(t+1)$ is the one-step ahead prediction of AFR which is regulated to $\lambda=1$. With selecting $n=1$ and $m = 2$, the RNFN controller has 14 inputs and one output:

$$= [1, AFR(t), \dots, AFR(t-n), P_{man}(t), P_{man}(t-1), \dots, P_{man}(t-m), rpm(t), rpm(t-1), \dots, x_{CA_{ip}} \quad (16)$$

$$rpm(t-m), a_{th}(t), a_{th}(t-1), \dots, a_{th}(t-m), t_{inj}(t-1), \dots, t_{inj}(t-m)];$$

$$u(t) = [t_{inj}(t)]$$

Process input output data obtained from the experimental test are then used to train the RNFNs. Based on Takagi-Sugeno modeling approach [42,48] each RNFN input is assigned to several fuzzy sets with the corresponding membership functions. Through logical combinations of the fuzzy inputs, the input space is clustered into several fuzzy regions. A local linear model is used within each region and the global model output is obtained through the defuzzification which is essentially the interpolation of local model outputs. Through training, membership functions of fuzzy operating regions are refined and local models are learned.

To build the RNFN estimator or controller, the real experimental data is partitioned into a training data set and a testing data set. In this work, 21994 data pairs ($x_{PA_{ip}}, y(t)$) in which $x_{PA_{ip}}$'s are the estimator inputs, have been partitioned into 16000 pairs for training and 5994 pairs for testing the RNFN estimator. While another arrangement of the same 21994 data in the form of ($x_{CA_{ip}}, u(t)$) pairs in which $x_{CA_{ip}}$'s are the controller inputs, have been divided to 16000 pairs for training and 5994 pairs for testing the RNFN controller. The training strategy is on the basis of back propagation algorithm and the network output is fed back to the network inputs through time delay units. During the training, both training error and testing error decrease. The appropriate point to stop training and to choose the membership function parameters is that point at which the test error is at its minimum. This procedure has been used to train both RNFN estimator and RNFN controller. The accuracy of the RNFN estimator is demonstrated by the small discrepancies between measured and predicted AFR, as shown in Figs. 11-14. Validating and effectiveness of the trained RNFN estimator is shown in Figures 15-18. As can be seen from these figures, the RNFN captures the AFR dynamics in the whole operating region very well.

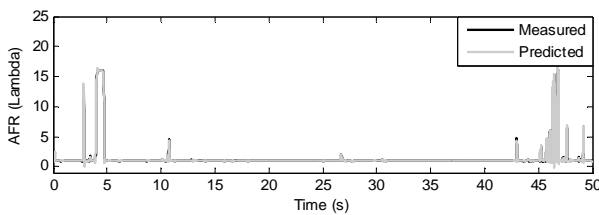


Fig. 11. Trajectories of measured and predicted AFR (Training Data Set)

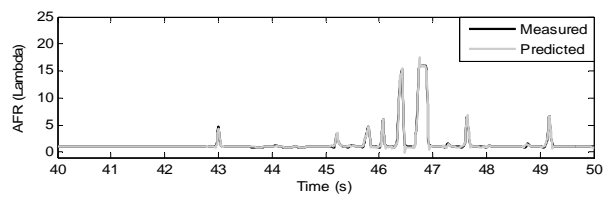


Fig. 12. Trajectories of measured and predicted AFR (Training Data Set) – Zoom (Time window (40,50))

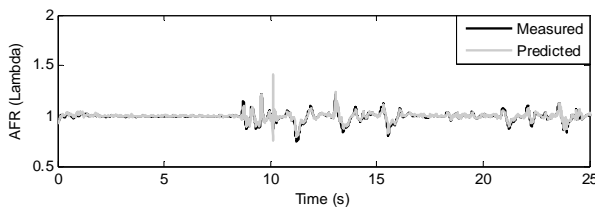


Fig. 13. Trajectories of measured and predicted AFR (Validating Data Set)

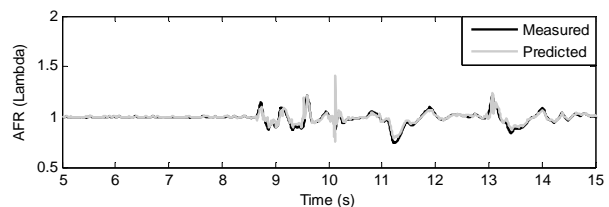


Fig. 14. Trajectories of measured and predicted AFR (Validating Data Set)- Zoom (Time window (5,15))

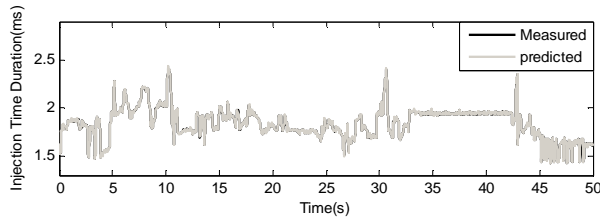


Fig. 15. Trajectories of measured and predicted Injection Time Duration (Training Data Set)

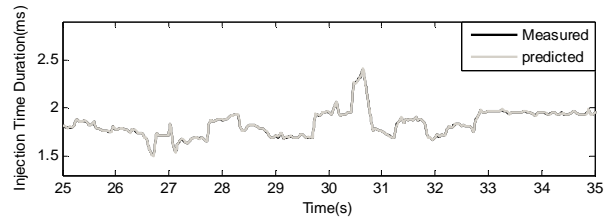


Fig. 16. Trajectories of measured and predicted Injection Time Duration (Training Data Set) – Zoom (Time window (25,35))

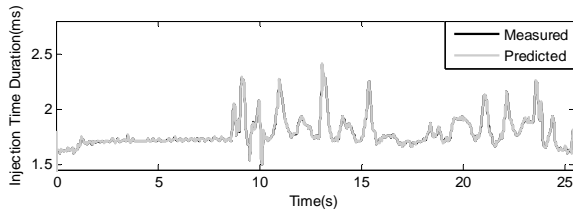


Fig. 17. Trajectories of measured and predicted Injection Time Duration (Validating Data Set)

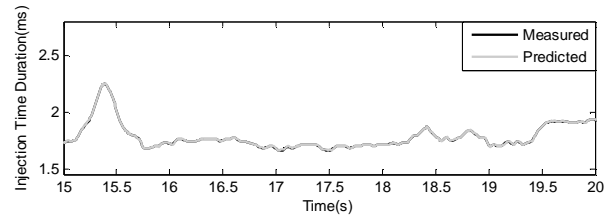


Fig. 18. Trajectories of measured and predicted Injection Time Duration (Validating Data Set) – Zoom (Time window (15,20))

7. CONCLUSION

Recurrent Neuro-Fuzzy Networks are proposed for building a nonlinear model/controller for AFR estimation/control of CNG-fueled engines. This type of nonlinear model/controller for the AFR is composed of several local linear models/controllers which are obtained by fuzzy clustering of engine operating region. The global model/controller output is obtained by combining local model/controller outputs based upon their membership functions. This RNFN estimation/control strategy utilizes both process knowledge and experimental process input output data. The experiments have been carried out on a real vehicle (Soren with EF7-TC engine) at the Engine Research Center of Irankhodro Company (IPCO). As the results show, such RNFN estimator/controller can model the AFR nonlinear dynamics/inverse dynamics with satisfactory accuracy. The advantages of this procedure are both the reduction in time consuming calibration efforts and the benefits of utilizing intelligent methods for AFR modeling and control.

Acknowledgment: The authors would like to acknowledge the great assistance of the Engine Research Center of Irankhodro Company (IPCO) in implementing the test scenario on a real vehicle and precisely collecting the required data.

REFERENCES

1. Barghi, F., Safavi, A. A. & Zarinchang, J. (2009). Reducing the vehicle environmental affects via modern control procedures. *Artificial Intelligence Journal*, pp. 18-21.
2. Barghi, F. & Safavi, A. A. (2011). An intelligent control policy for fuel injection control of SI engines (Case Study: CNG Engine). *15th IEEE International Conference on Intelligent Engineering Systems (INES 2011)*, Slovakia.
3. Guzzella, L. & Onder, Ch. (2004). *Introduction to modeling and control of internal combustion engine systems*. Springer-Verlag.
4. Kiencke, U. (1998) A view of automotive control systems. *IEEE Control Syst Mag*, Vol. 8, No. 4, pp. 11-18.
5. Zeng., K., Shiliang, L., Liu, B., Ma, F. & Huang, Z. (2006). Development and calibration on an electronic control system of CNG engine. *Vehicular Electronics and Safety, ICVES, IEEE*, pp. 204-208.

6. Jahirul, M. I., Masjuki, H. H., Saidur, R., Kalam, M. A., Jayed, M. H. & Wazed, M. A. (2010). Comparative engine performance and emission analysis of CNG and gasoline in a retrofitted car engine. *Applied Thermal Engineering*, Vol. 30, pp. 2219-2226.
7. Guzzella, L. & Onder, C. H. (2010). Introduction to modeling and control of internal combustion engine systems. *Springer-Verlag*, ISBN: 978-3-642-10774-0.
8. Xie, H., Stobart, R., Tunestal, P., Eriksson, L., Huang, Y. & Leteinturier, P. (2011). Engine control enabling environment friendly vehicle. *SAE Technical Paper 2011-01-0697*, USA.
9. Ursu, Ch., Bhat, R. & Damodaran, R. (2011). Simulink® modeling for vehicle simulator design. *SAE Technical Paper 2011-01-0746*, USA.
10. Linoa, P., Maionea, B. & Amoreseb, C. (2004). Modelling and predictive control of a new injection system for compressed natural gas engines. *Control Engineering Practice, Elsevier*, Vol. 16, pp. 1216–1230.
11. Guzzella, L. & Onder, Ch. (2004). Introduction to modeling and control of internal combustion engine systems. *Springer-Verlag*.
12. Moraal, P., Meyer, D., Cook, J. & Rychlick, E. (2000). Adaptive transient fuel compensation: Implementation and experimental results. *SAE Technical paper 2000-01-0550*.
13. Powell, J. D., Fekete, N. P. & Chang, C. (1998). Observer-based air-fuel ratio control. *IEEE Control System Mag.*, Vol. 18, pp. 72-83.
14. Chevalier, A., Vigild, C. W. & Hendricks, E. (2000). Predicting the port air mass flow of SI engines in air/fuel ratio control applications. *SAE Technical Paper 2000-01-0260*.
15. Choi, S. B. & Hendrick, J. K. (1998). An observer-based controller design method for improving air/fuel characteristics of spark ignition engines. *Transactions on Control Systems Technology*, Vol. 6, No. 3, pp. 325–334.
16. Vigild, C. W., Andersen, K. P. H. & Hendricks, E. (1999). Towards robust H-infinity control of an SI engine's air/fuel ratio. *SAE Technical Paper 1999-01-0854*.
17. Branstetter, M. (1999). Robust air-fuel ratio control for combustion engines. PhD Thesis, University of Cambridge.
18. Gene, Au. (2002). Linear parameter-varying modeling and robust control of variable cam timing engines. PhD Thesis, University of Cambridge.
19. Yoon, P. & Sunwoo, M. (2001). An adaptive sliding mode controller for air–fuel ratio control of spark ignition engines. *Proceedings of the Institution of Mechanical Engineers, Part D, Journal of Automobile Engineering*, Vol. 215, No. 10, pp. 305–315.
20. Wiens, T., Schoenau, G., Burton, R. & Sulatisky, M., Intelligent fuel air ratio control of gaseous fuel SI engines. Online: <http://homepage.usask.ca>.
21. Arsie, I., Di Iorio, S., Pianese, C., Rizzo, G. & Sorrentino, M. (2008). Recurrent neural networks for air-fuel ratio estimation and control in spark-ignited engines. *Proceedings of the 17th World Congress, The International Federation of Automatic Control*, Seoul, Korea.
22. Arsie, I., Marotta, M. M., Pianese, C. & Sorrentino, M. (2006). Experimental validation of a neural network based A/F virtual sensor for SI engine control. *SAE Technical paper 2006-01-1351*.
23. Arsie, I., Pianese, C. & Sorrentino, M. (2004). Nonlinear recurrent neural networks for air fuel ratio control in SI engines. *SAE Technical paper 2004-01-1364*.
24. Manzie, C., Palaniswami, M. & Watson, H. (2001). Gaussian networks for fuel injection control. *Proceedings of The Institution of Mechanical Engineers, Part D, Journal of Automobile Engineering*, Vol. 215, No. 10, pp. 1053–1068.
25. Manzie, C., Palaniswami, D., Ralph, M., Watson, H. & Yi, X. (2002). Model predictive control of a fuel injection system with a radial basis function network observer. *Journal of Dynamic Systems Measurement and Control, ASME*, Vol. 124, No. 4, pp. 648–658.

26. Lee, S. H., Walters, S. D. & Howlett, R. J. (2004). Engine fuel injection control using fuzzy logic, internal research, intelligent systems & signal processing laboratories. Engineering Research Center, University of Brighton, Moulsecoomb, Brighton, BN2 4GJ, UK.
27. Haj Bagheri, J., Alasti, A. & Safi Khani, A. (2004). Fuzzy control of air to fuel ratio of the internal combustion engine with manifold pressure observer. *Proceeding of the Third International Conference on Internal Combustion Engines*, Tehran, Iran.
28. Lauber, J., Guerra, T. M. & Dambrine, M. (2011). Air-fuel ratio control in a gasoline engine. *International Journal of Systems Science*, Vol. 42, No. 2, pp. 277-286.
29. Weige, Z., Jiuchun, J., Yuan, X. & Xide, Z. (2002). CNG engine air-fuel ratio control using fuzzy neural networks. *Proceedings of the 2nd International Workshop on Autonomous Decentralized System*, IEEE computer society Washington, DC, USA.
30. Yusaf, T. F., Buttsworth, D. R., Saleh, K. H. & Yousif, B. F. (2010). CNG-diesel engine performance and exhaust emission analysis with the aid of artificial neural network. *Applied Energy, Elsevier*, Vol. 87, pp. 1661-1669.
31. Allahbakhshi, M. & Akbari, A. (2011). Novel fusion approaches for the dissolved gas analysis of insulating oil. *Iranian Journal of Science and Technology, Transactions of Electrical Engineering*, Vol. 35, No. E1, pp. 13-24.
32. Semin Awang, I. & Rosli, A. B. (2009). Effect of port injection CNG engine using injector nozzle multi holes on air-fuel mixing in combustion chamber. *European Journal of Scientific Research*, ISSN: 1450-216X, Vol. 34, No. 1, pp. 16-24.
33. Pei Li, L. (2004). The effect of compression ratio on the CNG-diesel, engine. Bachelor thesis, University of Southern Queensland.
34. Barghi, F., Safavi, A. A. & Zarinchang, J. (2009). CNG fuel benefits for using in automotive. *Artificial Intelligence Journal*, ISSN: 1735-3939, pp. 47-51.
35. Bishop, C. M. (1995). *Neural networks for pattern recognition*. New York: Oxford University Press, pp. 116-160.
36. Hornik, K., Stinchcombe, M. & White, H. (1989). Multilayer feedforward networks are universal approximators, *Neural Networks*, pp. 359-366.
37. Kurkova, V. (1992). Kolmogorov's theorem and multilayer neural networks. *Neural Networks*, Vol. 5, No. 3, pp. 501-506.
38. Haykin, S. (1999). *Neural networks*. Prentice Hall.
39. Ertugrul, S. (2008). Predictive modeling of human operators using parametric and neuro-fuzzy models by means of computer-based identification experiment. *Engineering Applications of Artificial Intelligence*, Vol. 21, pp. 259-268.
40. Juang, C. F., Lin, C. T. (1999). A recurrent self-constructing neural fuzzy inference network. *IEEE Trans. Neural Networks*, Vol. 10, pp. 828-845.
41. Lee, C. H., Teng, C. C. (2000). Identification and control of dynamic systems using recurrent fuzzy neural networks. *IEEE Trans. Fuzzy Syst.*, Vol. 8, pp. 349-366.
42. Zhang, J. & Morris, A. J. (1999). Recurrent neuro-fuzzy networks for nonlinear process modeling. *IEEE Transactions on Neural Networks*, Vol. 10, No. 2.
43. Jang, J. R. (1993). ANFIS: adaptive-network-based fuzzy inference system, *IEEE Transactions on System, Man and Cybernetics*, Vol. 23, No. 3, pp. 665-685.
44. Jang, J. R. & Sun, C. T. (1995). Neuro-fuzzy modeling and control. *Proceedings of IEEE*, Vol. 83, No. 3, pp. 378-406.
45. Jang, J. R., Sun, C. T. & Mizutani, E. (1997). *Neuro-fuzzy and soft computing: a computational approach to learning and machine intelligence*. Prentice-Hall, New Jersey.
46. Wang, L. X. (1997). *A course in fuzzy systems and control*. Prentice-Hall.

47. Collins, T. (2008). XETKs provide cost-effective support of latest high speed ECU data acquisition needs, ETAS Inc.
48. Takagi, T. & Sugeno, M. (1985). Fuzzy identification of systems and its application to modeling and control. *IEEE Trans. Syst., Man, Cybern.*, SMC-15, pp. 116–132.